




Geology and Hydrogeophysical Investigation of Gurum and Environs, Lere Sheet 147SE, Bassa-Plateau, North-Central Nigeria

Y. B. Mohammed , Ilyasu Abdullahi Yerima, Aishatu Sani,
A. K. Gazali, Samaila B. Mshelia
Department of Geology, University of Maiduguri, Maiduguri, Nigeria

Suggested Citation

Mohammed, Y.B., Yerima, I.A., Sani, A., Gazali, A.K. & Mshelia, S.B. (2024). Geology and Hydrogeophysical Investigation of Gurum and Environs, Lere Sheet 147SE, Bassa-Plateau, North-Central Nigeria. *European Journal of Theoretical and Applied Sciences*, 2(2), 540-565.
DOI: [10.59324/ejtas.2024.2\(2\).47](https://doi.org/10.59324/ejtas.2024.2(2).47)

Abstract:

Geology and hydrogeophysical investigation of Gurum and its environs was undertaken within Lere Sheet 147 SE. The geological studies revealed the presence of Precambrian rocks (undifferentiated migmatites and Older Granites) and Jurassic rocks (Younger Granite) of different varieties belonging to the Buji Complex. The Buji Complex is composed of two (2) super imposed ring complexes, the earlier volcanic and high-level hyperbyssal intrusion dominated by granitic rocks. Hydrogeophysical results showed depth to various geo-electric layers and the range of apparent resistivity values with lithological units and their water yielding potentials. The studies clearly show the aquifer thickness is sufficient and the resistivity

value falls within the range of good water yield. Additionally, it can also be said that the aquifers in the study area including both weathered overburden and fractured crystalline rocks are capable of yielding significant amount of water to wells. The aquifer thickness appears to increase towards the north eastern part of Gurum.

Keywords: *Geology, Hydrogeophysical, Gurum, Bassa, Plateau.*

Introduction

The study area is located around Gurum and its environs within Lere Sheet 147 SE. The study area is underlain by the Precambrian rocks of the Nigerian Basement Complex as well as rocks belonging to the Younger Granite Suite. Here, groundwater occurs within the weathered overburden, as well as fractured crystalline rocks. These aquifer proportions vary from place to place. Geophysical investigation was carried out using schumberger array method in the collection of data, 10 VES points were taken in Gurum and its environment. The study was carried out to collate detail information about the hydrogeology of the area from the locals, to understand water related issues and develop

sustainable solutions in collaboration with the community. The data acquired provide a thorough understanding of the groundwater system on Gurum area, assisting in the sustainable development and management of water resources to meet the needs of the local population.

Additionally, geological and geophysical survey of Gurum and its environs was investigated, so as to ascertain the groundwater potential of the area in relation to its geology so as to achieve some of these specific objectives; to carry out detailed geological studies of the area, to determine resistivity values and thickness of various lithological rock units, and to also assess



the general water potential of the area in relation to rural water supply.

Location and Accessibility

The area of study is Gurum and its environs. It falls within the Basement Complex of North Central Nigeria consisting mainly of migmatite and the Younger Granites consisting of biotite granites belonging to the Buji Complex. The study area is bordered in the south by Mista Ali and in the north by Rumfar Gwamna Village, which are the major villages surrounding the study area. The study area has an estimated landmass of 20km² and lies between Latitudes 10°01'00"N to 10°02'35"N and Longitudes 8°48'15"E to 8°51'00"E (Fig. 1), provides an aerial photograph of the location of study area. The research area is accessible through Jos-Zaria road. Access through the research area was also made possible through a good network of secondary roads and footpaths that traverse. The accessibility of some parts of the area was hindered by the terrain which is hilly with high features and steep sides and the presence of gully

erosion in some areas. Figure 2 is the mean monthly rainfall of Jos area from 2010 to 2015. Table 1 also shows the mean monthly temperature of Jos- Plateau from 2010- 2015.



Figure 1. Aerial photograph of Location map of the study area Gurum, Bassa, Plateau State

Source: Google Earth Dr Mahadev Unde, Department of Electrical Engineering, Zeal College of Engineering and Research

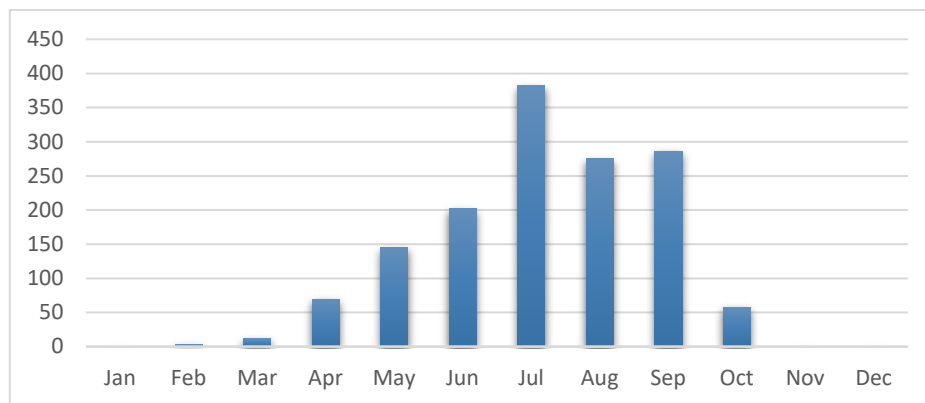


Figure 2: Mean Monthly Rainfall (mm) Chart for Stations in Jos, Plateau State from 2010-2015

Source: Observatory Station, Department of Geography and Planning, University of Jos

Table1. Temperature Data, Mean Monthly Temperature (°C) for station in Jos, Plateau State from 2010-2015

Month	Years						Mean monthly temperature
	2010	2011	2012	2013	2014	2015	
January	19	21	21	23	26	22.6	22.1
February	26.5	22	24	24.7	25	27	24.8
March	24.7	25	25	28.5	27	27.2	26.2
April	26.5	28	26.8	26	26	25.6	26.4
May	23.8	27	25.4	25	28	26.3	25.9

June	24.6	26	22.3	27.4	25.4	24.7	25.1
July	24.5	24	22.6	23.4	23.5	23.2	23.5
August	22.6	23	23.4	22.3	22.9	22.5	22.7
September	23.8	24	23	23	23.2	23.7	23.4
October	24.3	25	24.9	24	24.6	24.7	24.5
November	24.5	26	25	20	25.9	24	24.2
December	21.6	22	25	23	24.6	21	22.8
Mean temperature	23.8	24.4	24	24	25.2	24.4	24.3

Source: Observatory Station, Department of Geography and Planning, University of Jos (2010-2015)

Table 2. Rainfall Data, Mean Monthly Rainfall (mm) for Stations in Jos, Plateau State from 2010-2015

Month	Year						
	2010	2011	2012	2013	2014	2015	Mean rainfall
January	0.0	0.0	0.0	0.0	0.0	0.0	0.0
February	0.0	0.0	0.0	0.0	1.8	20.0	3.6
March	62.8	0.0	0.0	0.0	2.1	6.9	11.9
April	65.9	124.5	28.4	18.55	172.5	3.4	68.8
May	91.5	112.4	223.0	116.9	202.5	121.8	144.6
June	155.0	172.6	216.2	169.9	312.5	182.9	201.5
July	362.0	338.7	670.0	312.2	215.9	393.6	382.1
August	269.4	228.7	219.3	384.1	167.5	382.5	275.2
September	317.3	240.4	258.7	236.6	304.4	360.6	286.3
October	185.2	2.8	34.2	26.6	56.3	39.7	57.5
November	0.0	0.0	0.0	0.0	0.0	0.0	0
December	0.0	0.0	0.0	0.0	0.0	0.0	0

Source: Observatory, Department of Geography and Planning, University of Jos.

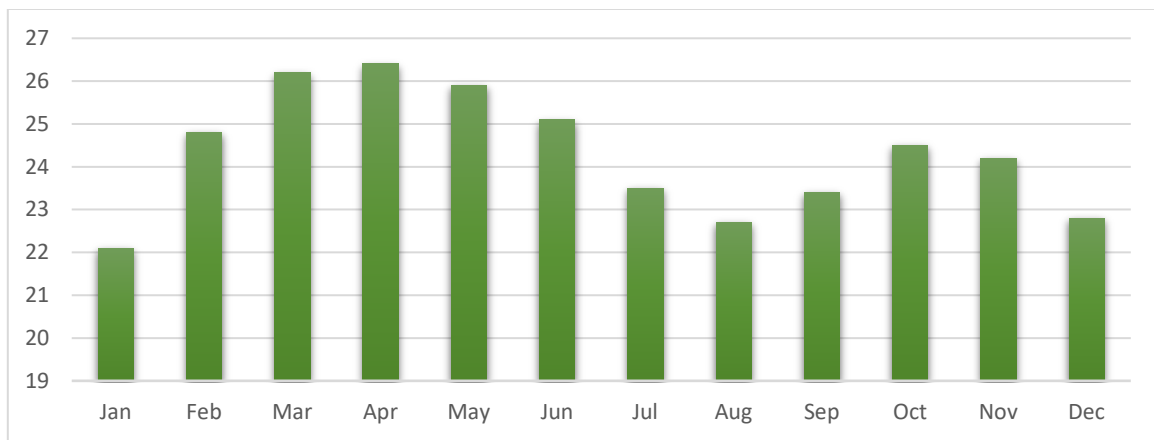


Figure 3. Mean Monthly Temperature(C°) Chart for Station in Jos, Plateau State from 2010-2015

Source: Observatory, Department of Geography and Planning, University of Jos.

The earliest study of the Buji Complex was done by Falconer (1911) in the survey of the Jos Plateau tin fields. The study was carried out on a

regional scale. Figure 4 below is a geological map of Nigeria showing the location of the Younger Granite rocks.

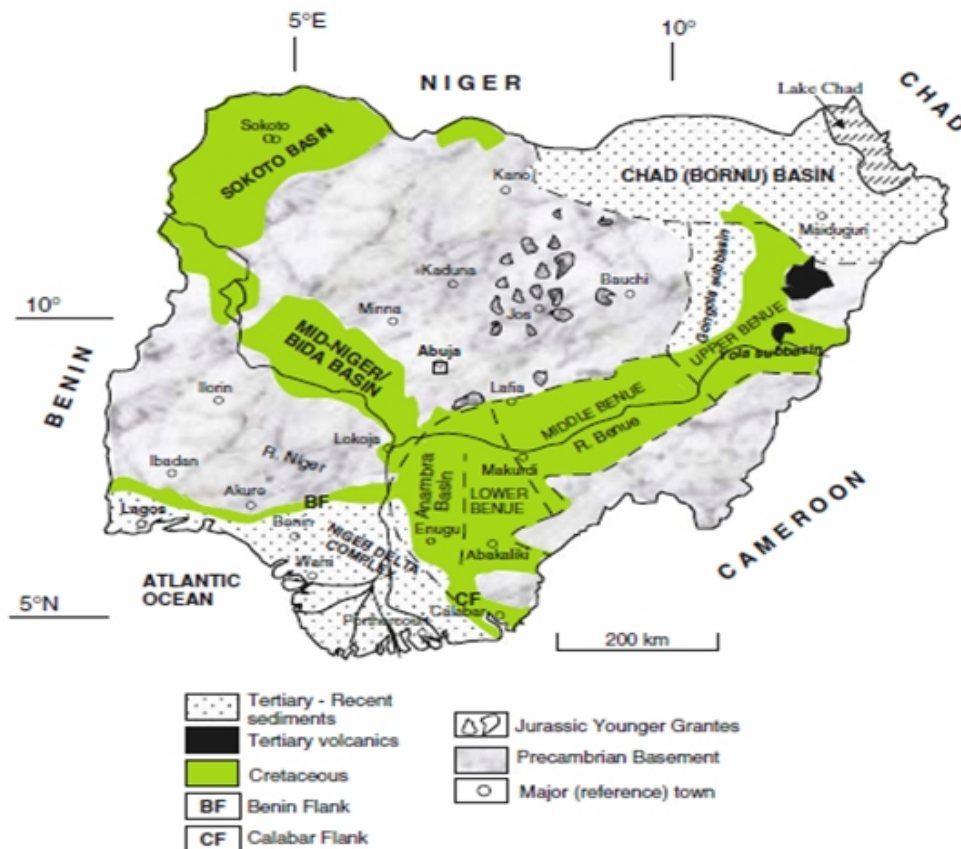


Figure 4. A simplified geologic map of Nigeria

Source: Obaje, 2009

Geology of Jos Plateau

The Jos Plateau area is a part of the Precambrian to Mid-Cambrian and Jurassic Northern Nigerian crystalline patches of Cenozoic Volcanic rocks, during the Pan-African as well as during the Early and Middle Cambrian, Older (Pan African) granites were emplaced in several places.

After a prolonged period of denudation, during the Jurassic, the second Phase of granites were intruded (Younger Granites) according to (Falconer, 1911). The Younger Granites of the Jos Plateau and surrounding areas are petrologically distinctive series of alkali feldspar granites associated with rhyolites and minor gabbros and syenites. They occur in sub-volcanic intrusive complexes as ring dykes and related annular and cylindrical intrusions. They

are richly mineralized with tin (Sn), niobium and columbite (Falconer, 1911).

The Younger Granites of the Jos Plateau occur as rocky hilly massifs sharply differentiated from the smoother topography of the surrounding basement rocks. In extent they cover an area of about 8600km² in central Nigeria and are located within a N-S rectangle of 400km long and 60km wide (Buchanan *et al.*,1971). It extends from south to north between Latitudes 9°00'N' to 10° 30'N and from the west to east between Longitudes 8°30'E to 9°30'E.

The Basement Complex rock underlies some two-third of the Jos Plateau. Wright (1971) gave a division of the Basement Complex rocks of Jos Plateau to include Pre-migmatite rocks, migmatites, granite gneiss and Older Granites. The description of the basement rock units presented below follows this division. Pre-

migmatite rocks are divided into granulitic gneiss and intermediate rocks. The granulitic gneisses are fine grained rocks with a sugary texture, grey to brown in colour, distinctly foliated and composed largely of quartz, feldspars and biotite (Wright, 1971). The usual rock type is a quartzo-feldspathic granulite with biotite either as dispersed flakes or aggregated in thin discontinuous bands or streaks parallel to the foliation. The gneisses may be uniform over extensive outcrops, modified only by thin veins of quartz or pegmatite.

Three groups of intermediate rocks occur on the Jos Plateau. These are the Rahaman diorite (located in extreme north-western part), the Toro diorite (located in the central part) and the Sho diorites located in south-western part. All the three possess a primary texture which compares with an igneous rock, modified by later crystalloblastic development chiefly of red brown biotite and microcline (Wright, 1971). The Rahaman and Toro diorites are hypsthene-bearing rocks and are wholly massive or almost so, while the Sho diorite contains hornblende and includes massive as well as foliated and strongly migmatized rocks with extensive neo-mineralization. The migmatites include rocks of varying lithologies, textures and structures, showing differing degrees of granitization and migmatization. They occupy mainly the western part of Jos Plateau. In general, exposure is limited and the outcrops are of low relief. Over large areas, the degree of migmatization may not change appreciably apart from local fluctuations, but generally there is a pronounced increase in the vicinity of the principal granites and granite gneiss masses.

Some of the migmatites are composite in nature, consisting of metamorphic host rock and acid injections which may be pegmatitic, feldspathic or granitic material (McCurry, 1989). In these composite migmatites, a discrete leucocratic component alternates with a more basic component (Wright, 1971). The migmatites are a varied group: ranging from coarsely mixed gneisses to more diffusely textured rocks of the variable grain size and frequently porphyroblastic. Foliation is usually not well marked but it is commonly shown by the streaky

aggregates of dark minerals which wind around the porphyroblastic feldspars. Metamorphism here is high grade. Granite gneiss, The term granite gneiss generally applied to a heterogeneous group of rocks, predominantly of granodioritic composition, in which variable amounts of remnant streaks and larger relict bodies of original gneiss are recognizable, and in which subordinate granitic and tonalitic phases occur (McCurry, 1989). On the Jos Plateau they occur in north-central, north-eastern, eastern and south-eastern parts, Where the rock have contacts with migmatites, they are transitional and generally have a complete structural conformity with the foliation in both rocks trending parallel to the common boundary (Wright, 1971). The main component minerals of the granite gneisses are plagioclase, quartz, microcline, and biotite. The common accessories include apatite, epidote, muscovite, sericite sphene, allanite and iron ore.

Older Granites encompass rocks intruded during the Pan-African orogenic cycle (McCurry, 1989). Three main categories were identified, based largely on general texture and mineralogical characteristics, are recognized on the Jos Plateau area. The first group is most extensive and include medium to coarse grained biotite and biotite hornblende granites which are frequently porphyritic. These occur in patches as inselbergs on the Plateau and include and the Dass Hills granite (located at the eastern part). Others are the Zagun Granite (located in the western part), the Maijuju and the Sho Granite found in the central and south-western parts respectively.

The Second group is the medium to coarse grained biotite hornblende granites and quartz syenites. They are mostly non-porphyritic and outcrop mainly in the south-eastern and north-central parts of the Jos Plateau as Gindiri Granite and part of the Toro Annular Complex, respectively. They are composed of feldspars, quartz, biotite and hornblende.

The third group is fine to medium-grained and biotite-muscovite granites. They are widely distributed but are mostly concentrated in the western and south-western parts of the Jos

Plateau. These granites are found outcropping within the Maijuju and Gora Granite in the central part and the Gindiri Granite and Lere Granite in the south-eastern part. Other outcrops of this rock type include those of the Assob Granite (located in the south-western part), the Rafin Bauna Granite and the Mariri Granite all located in the western part of the Jos Plateau. They are composed mainly of biotite and muscovite and are distinguished by large crystal of sphene.

The Younger Granites of Jos the Plateau occupy about one-third of the total surface area. The granites were first defined by Falconer (1911). He described them as cross-cutting alkali granites of reibeckite or biotite characterized by chilled margins against their country rocks. As they are known today, the rocks occur as hilly massifs sharply differentiated from the smoother topography of the surrounding basement rocks. They are petrologically distinctive series of alkali feldspar granites, associated with rhyolites and minor gabbros and syenites, which occur in sub-volcanic intrusive complexes as ring dykes and related annular and cylindrical bodies (Turner, 1976).

Younger Granite complexes consist of a series of distinct intrusions often having a concentric arrangement, each intrusion having petrographic features which occur in a province. According to MacLeod *et al.* (1971), the rock types of the complexes include rhyolites, granites, syenites and basic rocks. There are two kinds of rhyolite on the Jos Plateau, namely Early and Late rhyolites. The Early rhyolites display a greater diversity of texture; they have porphyritic glassy and spherulitic varieties. They usually contain iron oxides, amphibole, pyroxene, sparse quartz and alkali feldspar. Phenocrysts in finely crystalline matrix also occur in this variety. Late rhyolites consist of very abundant phenocrysts of quartz and alkali feldspar, often fractured and aggregated. They are remarkably uniform in texture, both laterally and vertically. The granites are constant in character throughout the province although they exhibit a large variety of rock types. The granite suite comprises hornblende granite and porphyries group, biotite and reibeckite granites. The hornblende granite

and porphyries group contains a wide range of colored minerals including fayalite, hedenbergitic pyroxene, hornblende, arfvedsonite and biotite. The hornblende granite sometimes appears as large plutons with granite texture, but in the ring dykes, they commonly assume a porphyritic texture, and to this facies, the term granite porphyry is applied (MacLeod and Turner, 1971). In the Jos Plateau, the early ring dykes are frequently of a coarse hornblende-biotite-granite of granite porphyry and this rock type is also abundant as plutons. The biotite-granite is the most abundant and widespread rock type on the Plateau. They form some of the largest individual intrusions (MacLeod and Turner, 1971), and contain a wide variety of interesting accessory minerals which include zircon, fluorite and iron oxides, thorite, monazite and xenotime (Turner, 1976).

Syenites have a wide distribution in the Younger Granite Province but cover a comparatively small area. The most extensive occurrence is at the north-eastern corner of the province. They have both granular and porphyritic texture (MacLeod and Turner (1971). The main component is alkali feldspar but some syenites contain minor plagioclase. Common accessory minerals include ilmenite, zircon, apatite, calcite and allanite.

Basic rocks appear in many of the complexes but are always in the form of small intrusions which have-preceded the granites and have been partly obliterated. The rocks occur in the form of gabbros, dolerites and basalts. The typical gabbro is a coarse grained rock composed of basic plagioclase, hornblende, augite, occasionally olivine and accessory iron oxide; the gabbro intrusions are usually composite masses and include medium- fine grained facies (MacLeod and Turner, 1971). Basic rock in the form of dolerite and basalts occur as lava flows, dykes and semi-concordant intrusions in the rhyolites and granites of many of the complexes. Some precede the granite but, there is abundant evidence for the recurrence of basic intrusion at all stages of the acid cycle (MacLeod and Turner, 1971).

Geology of the Study Area

The Gurum area and its environs lie within the Buji area. The area is underlain both by undifferentiated migmatites and Older Granite, as well as in part by Younger Granite belonging to the Buji Complex. The Buji Complex forms a part of the Northern Nigeria Younger Granite Ring Complex, which are a part of the larger igneous province extending from Afu in Nigeria to as far to the north in Niger republic. The Buji Complex is generally circular in outline covering an area of about 48km² with a maximum diameter of about 10km. This complex forms a high dissected Plateau in the northern part, of which Dutsen Buji (1170.74m) forms the highest point, the southern area of the Buji Complex is of more subdued topography with low rocky hills around.

The Buji Massif is composed of two (2) super imposed ring complexes, the earlier being the eastern ring complex composed almost entirely of volcanic rocks and high-level hyperbyssal intrusion, while the western ring complex is the later and is dominated by granitic rocks. However both ring complexes have a related mode of emplacement (i.e. the tectonic process that was associated with the epirogenic uplift).

The volcanic activities are marked by two (2) stages; the patterns of both are controlled by essentially the same tectonic processes that control the emplacement of the granite plutons and ring-dykes at greater depth. The earlier stage being the development of vent along the line of ring fault, the later being marked by segmental fracturing and differential subsidence, containing mainly the Early and Late Rhyolites Macleod *et al.* (1971)

Quartz-hedenbergite porphyry has been introduced into the Late Rhyolite and also a ring dyke of quartz feldspar-porphyry has been emplaced in the complex. A comparatively simple pattern granite ring- structure occupies the western half of the complex, the emplacements of which was preceded by the intrusion of cone-sheets which cuts the rhyolites and the Basement Complex on the eastern and the northern sides of the granite. A discontinuous ring-dyke of aegirine-micro-

granite has followed the cone sheets, which in turn has been partly obliterated by the main intrusion of biotite granite. At the western side of the complex albite- riebeckite granite are also found.

This study essentially involved the use of geophysics to determine the aquifer geologic characteristics in relation to the water yielding potentials. To be aquiferous, the subsurface rocks must be sufficiently weathered or fractured for improved porosity.

Groundwater tends to be highly limited in extent in basement and other crystalline rock terrains (Olorunfemi *et al.*, 1999; Offodile, 2002). Thereby a subsurface method of finding water is important. There are many important geophysical techniques used in groundwater exploration, like gravity, magnetic, seismic refraction, and geo-electrical prospecting methods. Out of this, electrical resistivity method helps in solving groundwater problems through its highest resolving power and economical viability. Electrical resistivity methods are used to investigate the different lithological formations, bed rock dispositions, the depth to water table or zone of saturated formations, thickness of weathered zones, detection of fissures, fractures, and fault zones, establishment of their depths, thickness and lateral extent of aquifer.

Materials and Methods

Principles of Electrical Resistivity Survey

Electrical resistivity survey was employed in this research by passing a known electric current into the ground by means of two current electrodes and the potential differences between the other two potential electrodes is measured. The potential variations may be change due to size, shape and conducting capacity of the material in the subsurface and from the quantities of potential differences and the current applied where the resistance is calculated. Electrical resistivity can be termed in ohm- meter recorded as a standard unit. Electrical Resistivity Surveys could find out a good electrical resistivity difference between the water bearing formations

and the surrounding rocks can be achieved using software (Zohdy *et. al.*, 1974). In this process a known value of electric current (I) is passed into the ground by two outer metals stakes (C1 and C2) that are buried in the ground. The potential variation (V) is measured between two inner electrodes termed potential electrodes (P1 and P2).

The ratio of V/I provides the resistance (R) and by multiplying R with the geo-electrical factor (K) of the electrode separation, the resistivity 'ρ', and it is inverse of conductivity of the ground may be described.

$$\text{Resistance (R)} = V/I$$

$$\text{Resistance(R)} \times \text{geo-electric factor (K)} = \text{resistivity}$$

The potential variation passes because of the externally pressing current between various electrodes, the apparent resistivity of the elements established in the given geologic formation which does not match the average resistivity and it may be lower than the lowest and higher than the highest resistivity within the subsurface to which it pertains. The apparent potential value of 'ρ' corresponds to the true resistivity, if the ground is homogeneous and isotropic when it is obtained from the measurements over a layered or heterogeneous ground, then it is only an apparent resistivity and is signed by 'ρ_a', the quality being used in the interpretation of electrical methods.

The resistivity of geological subsurface formations differs very broadly not only from formation to formation but also within one lithological unit and is related to

- Size and shape of the aquifer materials, density, porosity, pore size of the material
- Quality of water, size, shape, pore space and density of the aquifer horizons
- Distribution of water in the rocks due to the structural and textural characteristics and

- The temperature of the subsurface of the water environment.

Many different electrode arrangements have been proposed and used for resistivity exploration. Wenner Schlumberger and Axial Dipole-Dipole arrangements are widely used because the interpretation tools are well developed and they will be adequate for application to groundwater and shallow geologic problems. The Schlumberger arrangement is widely used for quantitative interpretation in Vertical Electrical Sounding compared with Wenner. It offers the important advantage of being less sensitive to unknown lateral homogeneities because the potential electrode (M & N) remains in fixed position during a large number of sensitive measurements.

Data is collected using standard electrode configuration of schlumberger configuration using the principal that the current electrodes vary along a straight line in both directions. However, the potential electrodes remain constant and moved when better results of subsurface strata is needed in case of weak signals. Four electrodes are placed along a straight line on the Earth's surface in the same order, AMNB, as in the Wenner array, but with $AB \geq 5 MN$.

Field geophysical measurements were carried out using the vertical electrical sounding (VES) technique and using the Allied Omega Terrameter as the field operating equipment as shown in Plate 1. The maximum electrical spread was (AB/2) was 125 meters.

With a Schlumberger array the various resistance values obtained from the Terrametre for the various AB/2 points were multiplied by the different K-factors to obtain various electrode spacing AB/2 values were then plotted against the apparent resistivity values using the Zohdy geophysical software which produced the geophysical curves as well as the processed data. The sounding sites were selected across the area especially within the various settlements. In all, ten (10) vertical electrical soundings VES points were made within the study area.

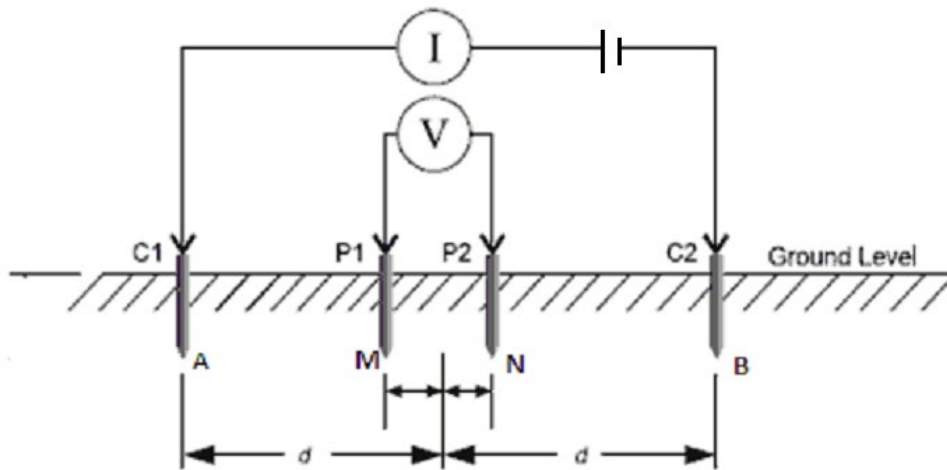


Figure 5. The Schlumberger Array



Figure 6. Resistivity Metre

Results

The electrode space ($AB/2$) in metres, resistance and apparent resistivity data obtained in the field, as well as the processed data obtained using the Zohdy geophysical software and are presented in

Tables 3 (a&b) to 12 (a&b). Tables 3b to 12b are the processed data from which the depth to various lithostratas as well as the geophysical nature of the rock materials below each VES where obtained. Details of the interpretation of the results are presented.

Table 3a. Field Geophysical Data for VES 1

S/NO	AB/2(metres)	K	RESISTANCE(ohms)	APPARENT RESISTIVITY(ohm-m)
1	1.5	6.28	240.2	1508.46
2	2.0	11.78	121.8	1434.80
3	2.6	20.45	46.71	955.22
4	3.4	35.5	18.88	670.24
5	4.5	62.8	6.468	406.19
6	6.0	112.3	2.711	304.45
7	8.0	200	0.9027	180.54
8	10.5	346	0.3567	123.43
9	14.0	615	0.1553	95.51
10	10.5	44	7.24	318.56
11	14.0	82.5	2.528	208.56
12	18.0	140	1.015	142.1
13	24.0	253	0.2985	75.52
14	32.0	454	0.2543	115.68
15	42.0	786	0.1401	110.12
16	55.0	1352	0.06742	91.15
17	42.0	176	0.7633	134.34
18	55.0	317	0.445	141.07
19	72.5	568	0.2716	154.27
20	95.0	991	0.1794	177.79
21	125.0	1730	0.1358	234.93

Table 3b Processed Geophysical Data for VES 1

S/No	Depth(m)	Resistivity(ohm.m)	S/No	Depth(m)	Resistivity(ohm.m)
1	0.99	7712.01	7	9.91	183.02
2	1.45	2776.46	8	14.54	97.98
3	2.13	1125.74	9	21.35	125.95
4	3.13	892.45	10	31.33	122.58
5	4.60	774.71	11	45.99	139.61
6	6.75	479.11	12	99999.0	316.75

Table 4a. Field Geophysical Data for VES 2

S/NO	AB/2(metres)	K	RESISTANCE(ohms)	APPARENT RESISTIVITY(ohm-m)
1	1.5	6.28	63.15	396.58
2	2.0	11.78	30.26	356.46
3	2.6	20.45	14.01	286.51
4	3.4	35.5	7.21	255.96
5	4.5	62.8	3.818	239.77
6	6.0	112.3	1.858	208.66
7	8.0	200	0.8672	173.44
8	10.5	346	0.4356	150.72
9	14.0	615	0.2122	130.50
10	10.5	44	4.661	305.09
11	14.0	82.5	2.173	179.27
12	18.0	140	1.137	159.18
13	24.0	253	0.6631	167.76
14	32.0	454	0.3645	165.48
15	42.0	786	0.2345	184.32
16	55.0	1352	0.1401	189.42
17	42.0	176	1.652	290.76
18	55.0	317	0.8241	261.24

19	72.5	568	0.5443	309.17
20	95.0	991	0.3317	328.72
21	125.0	1730	0.188	325.24

Table 4b Processed Geophysical Data for VES 2

S/No	Depth(m)	Resistivity(ohm.m)	S/No	Depth(m)	Resistivity(ohm.m)
1	0.89	879.18	7	8.92	175.76
2	1.31	499.62	8	13.98	176.77
3	1.92	422.84	9	19.21	216.16
4	2.82	439.09	10	28.20	288.25
5	4.14	368.01	11	41.39	359.10
6	6.080	241.48	12	99999.00	376.31

Table 5a. Field Geophysical Data for VES 3

S/NO	AB/2(metres)	K	RESISTANCE(ohms)	APPARENT RESISTIVITY(ohm-m)
1	1.5	6.28	34.40	216.16
2	2.0	11.78	15.84	186.62
3	2.6	20.45	8.936	183.75
4	3.4	35.5	4.904	174.10
5	4.5	62.8	2.295	144.13
6	6.0	112.3	1.34	150.49
7	8.0	200	0.7362	147.24
8	10.5	346	0.4112	142.28
9	14.0	615	0.2599	159.84
10	10.5	44	4.774	210.06
11	14.0	82.5	2.666	219.95
12	18.0	140	1.723	241.22
13	24.0	253	0.9467	239.52
14	32.0	454	0.5585	253.56
15	42.0	786	0.2321	182.43
16	55.0	1352	0.0921	124.52
17	42.0	176	1.145	201.52
18	55.0	317	0.6589	208.88
19	72.5	568	0.3881	220.50
20	95.0	991	0.2554	253.11
21	125.0	1730	0.3152	545.30

Table 5b. Processed Geophysical Data for VES 3

S/No	Depth(m)	Resistivity(ohm.m)	S/No	Depth(m)	Resistivity(ohm.m)
1	0.99	482.26	7	9.91	543.69
2	1.45	426.25	8	14.54	639.97
3	2.13	336.09	9	21.35	348.27
4	3.13	276.66	10	31.33	101.99
5	4.60	269.34	11	45.99	99.79
6	6.75	348.76	12	99999.00	950.52

Table 6a. Field Geophysical Data for VES 4

S/NO	AB/2(metres)	K	RESISTANCE(ohms)	APPARENT RESISTIVITY(ohm-m)
1	1.5	6.28	125.6	788.77
2	2.0	11.78	64.16	755.81
3	2.6	20.45	38.58	788.97

4	3.4	35.5	19.90	706.45
5	4.5	62.8	7.89	495.50
6	6.0	112.3	3.351	376.32
7	8.0	200	1.563	312.60
8	10.5	346	0.7626	263.86
9	14.0	615	0.4092	251.66
10	10.5	44	9.83	432.52
11	14.0	82.5	5.016	413.82
12	18.0	140	2.752	385.28
13	24.0	253	1.218	308.16
14	32.0	454	0.5311	241.12
15	42.0	786	0.2762	217.10
16	55.0	1352	0.1452	196.31
17	42.0	176	0.218	214.37
18	55.0	317	0.6387	202.47
19	72.5	568	0.4102	233.00
20	95.0	991	0.3026	299.88
21	125.0	1730	0.1736	300.33

Table 6b. Processed Geophysical Data for VES 4

S/No	Depth(m)	Resistivity(ohm.m)	S/No	Depth(m)	Resistivity(ohm.m)
1	0.89	1320.35	7	8.92	570.18
2	1.31	1886.69	8	13.09	364.56
3	1.92	1409.23	9	19.21	148.31
4	2.82	589.83	10	28.20	121.44
5	4.14	320.63	11	41.39	220.36
6	6.08	427.74	12	99999.0	409.06

Table 7a. Field Geophysical Data for VES 5

S/NO	AB/2(metres)	K	RESISTANCE(ohms)	APPARENT RESISTIVITY(ohm-m)
1	1.5	6.28	258.4	1622.76
2	2.0	11.78	128.7	1516.09
3	2.6	20.45	77.14	1577.52
4	3.4	35.5	38.21	1356.46
5	4.5	62.8	17.33	1088.33
6	6.0	112.3	6.984	784.31
7	8.0	200	2.503	500.6
8	10.5	346	1.023	353.96
9	14.0	615	0.592	364.08
10	10.5	44	11.47	504.48
11	14.0	82.5	4.356	359.37
12	18.0	140	2.293	309.82
13	24.0	253	1.104	279.32
14	32.0	454	0.5494	249.43
15	42.0	786	0.297	233.45
16	55.0	1352	0.1753	237.01
17	42.0	176	1.431	151.86
18	55.0	317	0.7565	239.81
19	72.5	568	1.665	945.72
20	95.0	991	0.2325	230.41
21	125.0	1730	0.2955	511.22

Table 7b. Processed Geophysical Data for VES 5

S/No	Depth(m)	Resistivity(ohm.m)	S/No	Depth(m)	Resistivity(ohm.m)
1	0.89	1443.98	7	8.92	434.36
2	1.31	2350.63	8	13.09	257.83
3	1.92	2081.96	9	19.21	133.59
4	2.82	836.36	10	28.20	199.83
5	4.14	246.85	11	41.39	465.87
6	6.08	246.67	12	99999.0	984.39

Table 8a. Field Geophysical Data for VES 6

S/NO	AB/2(metres)	K	RESISTANCE(ohms)	APPARENT RESISTIVITY(ohm-m)
1	1.5	6.28	204.7	1285.52
2	2.0	11.78	94.27	1110.5
3	2.6	20.45	39.02	797.96
4	3.4	35.5	18.85	669.18
5	4.5	62.8	8.291	520.67
6	6.0	112.3	4.703	528.15
7	8.0	200	2.382	476.46
8	10.5	346	1.358	469.87
9	14.0	615	0.597	367.16
10	10.5	44	11.17	491.48
11	14.0	82.5	4.62	381.15
12	18.0	140	2.873	402.22
13	24.0	253	1.869	472.86
14	32.0	454	0.6113	277.53
15	42.0	786	0.3381	265.75
16	55.0	1352	0.2081	281.36
17	42.0	176	4.267	751.00
18	55.0	317	2.98	944.66
19	72.5	568	0.6487	368.47
20	95.0	991	0.9863	977.43
21	125.0	1730	0.8018	1387.12

Table 8b. Processed Geophysical Data for VES 6

S/No	Depth(m)	Resistivity(ohm.m)	S/No	Depth(m)	Resistivity(ohm.m)
1	0.99	5752.27	7	9.91	1559.76
2	1.45	2100.62	8	14.54	1699.04
3	2.13	1279.53	9	21.35	1045.32
4	3.13	1611.61	10	31.33	357.66
5	4.60	1634.31	11	45.99	277.69
6	6.75	1378.26	12	99999.00	2033.83

Table 9a. Field Geophysical Data for VES 7

S/NO	AB/2(metres)	K	RESISTANCE(ohms)	APPARENT RESISTIVITY(ohm-m)
1	1.5	6.28	412.5	2590.50
2	2.0	11.78	154.3	1817.66
3	2.6	20.45	70.06	1432.73
4	3.4	35.5	28.33	1005.72
5	4.5	62.8	13.50	847.80
6	6.0	112.3	7.453	836.98
7	8.0	200	2.934	586.80
8	10.5	346	4.803	1661.84

9	14.0	615	2.234	1373.91
10	10.5	44	17.16	755.04
11	14.0	82.5	7.301	602.34
12	18.0	140	3.787	530.18
13	24.0	253	1.553	392.91
14	32.0	454	0.4671	212.06
15	42.0	786	0.2386	187.54
16	55.0	1352	0.2934	396.68
17	42.0	176	1.35	237.60
18	55.0	317	0.6011	190.55
19	72.5	568	0.3973	225.67
20	95.0	991	0.2595	257.17
21	125.0	1730	0.07369	127.8

Table 9b. Processed Geophysical Data for VES 7

S/No	Depth(m)	Resistivity(ohm.m)	S/No	Depth(m)	Resistivity(ohm.m)
1	0.80	620.60	7	8.03	437.65
2	1.18	343.19	8	11.78	229.01
3	1.73	140.88	9	17.29	80.30
4	2.54	85.82	10	25.38	78.78
5	3.72	156.61	11	37.25	176.12
6	5.47	354.41	12	99999.00	163.85

Table 10a. Field Geophysical Data for VES 8

S/NO	AB/2(metres)	K	RESISTANCE(ohms)	APPARENT RESISTIVITY(ohm-m)
1	1.5	6.28	94.44	593.09
2	2.0	11.78	45.08	531.05
3	2.6	20.45	17.26	352.97
4	3.4	35.5	9.972	354.01
5	4.5	62.8	5.91	371.15
6	6.0	112.3	3.361	377.44
7	8.0	200	3.016	603.20
8	10.5	346	1.452	502.40
9	14.0	615	0.7189	442.13
10	10.5	44	7.663	337.44
11	14.0	82.5	3.406	281.00
12	18.0	140	1.621	226.94
13	24.0	253	0.5869	142.49
14	32.0	454	0.3071	139.43
15	42.0	786	0.08271	65.01
16	55.0	1352	0.0433	58.55
17	42.0	176	0.2807	49.41
18	55.0	317	0.2686	85.15
19	72.5	568	0.1936	109.95
20	95.0	991	0.1084	107.43
21	125.0	1730	0.07733	133.78

Table 10b. Processed Geophysical Data for VES 8

S/No	Depth(m)	Resistivity(ohm.m)	S/No	Depth(m)	Resistivity(ohm.m)
1	0.80	804.91	7	8.03	610.28
2	1.18	216.07	8	11.78	268.65
3	1.73	170.55	9	17.29	73.86
4	2.54	333.04	10	25.38	43.38

5	3.72	618.13	11	37.25	80.05
6	5.47	771.55	12	99999.00	164.92

Table 11a. Field Geophysical Data for VES 9

S/NO	AB/2(metres)	K	RESISTANCE(ohms)	APPARENT RESISTIVITY(ohm-m)
1	1.5	6.28	30.36	190.66
2	2.0	11.78	17.56	206.86
3	2.6	20.45	11.27	230.48
4	3.4	35.5	7.037	249.82
5	4.5	62.8	3.909	245.49
6	6.0	112.3	2.031	228.09
7	8.0	200	0.999	199.80
8	10.5	346	0.5361	185.49
9	14.0	615	0.2934	180.45
10	10.5	44	5.534	243.50
11	14.0	82.5	2.894	238.76
12	18.0	140	1.706	238.84
13	24.0	253	0.8671	218.12
14	32.0	454	0.3919	177.93
15	42.0	786	0.2102	165.25
16	55.0	1352	0.1218	164.68
17	42.0	176	0.9819	172.82
18	55.0	317	0.5524	175.11
19	72.5	568	0.3473	197.27
20	95.0	991	0.2345	232.39
21	125.0	1730	0.1645	284.59

Table 11b. Processed Geophysical Data for VES 9

S/No	Depth(m)	Resistivity(ohm.m)	S/No	Depth(m)	Resistivity(ohm.m)
1	0.89	223.62	7	8.9	299.23
2	1.31	458.77	8	13.092	304.16
3	1.92	581.89	9	19.21	134.94
4	2.82	402.94	10	28.20	81.32
5	4.14	211.38	11	41.39	160.88
6	6.08	186.76	12	99999.00	549.26

Table 12a. Field Geophysical Data for VES 10

S/NO	AB/2(metres)	K	RESISTANCE(ohms)	APPARENT RESISTIVITY(ohm-m)
1	1.5	6.28	37.77	237.26
2	2.0	11.78	19.09	224.88
3	2.6	20.45	11.77	240.70
4	3.4	35.5	6.905	245.13
5	4.5	62.8	3.523	221.25
6	6.0	112.3	1.716	192.71
7	8.0	200	0.8195	163.90
8	10.5	346	0.3919	135.60
9	14.0	615	0.1848	113.66
10	10.5	44	5.281	232.37
11	14.0	82.5	2.372	195.69
12	18.0	140	1.216	170.24
13	24.0	253	0.6344	157.98
14	32.0	454	0.3122	141.74
15	42.0	786	0.1645	129.30

16	55.0	1352	0.0909	122.87
17	42.0	176	0.6406	112.75
18	55.0	317	0.4064	128.83
19	72.5	568	0.2716	154.27
20	95.0	991	0.1865	184.83
21	125.0	1730	0.1076	186.15

Table 12b. Processed Geophysical Data for VES 10

S/No	Depth(m)	Resistivity(ohm.m)	S/No	Depth(m)	Resistivity(ohm.m)
1	0.89	387.76	7	8.92	184.16
2	1.31	515.20	8	13.09	149.64
3	1.92	540.19	9	19.21	98.04
4	2.82	421.59	10	28.20	100.48
5	4.14	275.69	11	41.39	157.65
6	6.08	199.43	12	99999.00	237.87

Data Interpretation

Results were obtained in the form of geophysical curves and apparent resistivity is plotted against the different depths. Geophysical curves obtained, as shown in Figures 6 to 15, are of different types. They include:

QH- VES 1, 5 and 7

H- VES 2, 10

KH- VES 3, 7, 8

HKH- VES 4, 6 and 9

Geophysical sounding curves can be of different types depending on the geological and hydrogeological environment. If the ground is composed of two layers the curves are of two types i.e. (1) Ascending type (2) Descending type. The ascending type of curves are established where the ground has a two-layer structure, the topsoil or weathered layer and hard compact basement (high resistivity). The descending type of curves are established where a top layer is overlying a thick clay or saline water aquifer.

If the ground is composed of three layers of resistivities ρ_1, ρ_2, ρ_3 and thicknesses $h_1, h_2,$ and $h_3 = \infty$, the geo-electric section is described according to the relation between the values of ρ_1, ρ_2, ρ_3 . There are four possible combinations between the values of ρ_1, ρ_2, ρ_3 . These are;

- 1) $\rho_1 > \rho_2 < \rho_3$ H-type curve (minimum type)
- 2) $\rho_1 < \rho_2 < \rho_3$ A-type curve (ascending type)
- 3) $\rho_1 < \rho_2 > \rho_3$ K-type curve (maximum type)
- 4) $\rho_1 > \rho_2 > \rho_3$ Q-type curve (descending type)

Types H and K curves have a definite minimum and maximum, indicating a bed or beds of anomalously low or high resistivity respectively at intermediate depth. Types A and Q curves show fairly uniform change in resistivity, the first increasing the second decreasing with depth.

A-type curves are obtained in the hard rock environments with conductive topsoil. In this case, the resistivity of the layers will be continuously increasing ($\rho_1 < \rho_2 < \rho_3$). Sounding curves which have maximum peak and are occupied by low resistivity values ($\rho_1 < \rho_2 > \rho_3$) are termed K-type curves and such curves result from different environment. A sounding curve with continuously decreasing resistivity ($\rho_1 > \rho_2 > \rho_3$) is said to be Q-type curve and this type of curves are commonly obtained in coastal region because of the saline water. The sounding curves with a central minimum ($\rho_1 > \rho_2 < \rho_3$) are called H-type curves. This type of sounding curves are normally found in hard rock formations and it consists of a dry top soil of high resistivity as the first layer, water saturated weathered layer of minimum resistivity as the

second layer and compact hard rock unit with a very high resistivity as the third layer.

If the ground is composed of more than three horizontal layers of resistivities $\rho_1, \rho_2, \rho_3, \dots, \rho_n$ and thicknesses $h_1, h_2, h_3, \dots, h_n = \infty$, the

geo-electric section is described in terms of the relationship between the resistivities of the layers, and the letters H, A, K and Q are used in combination to indicate the variation of resistivity with depth.

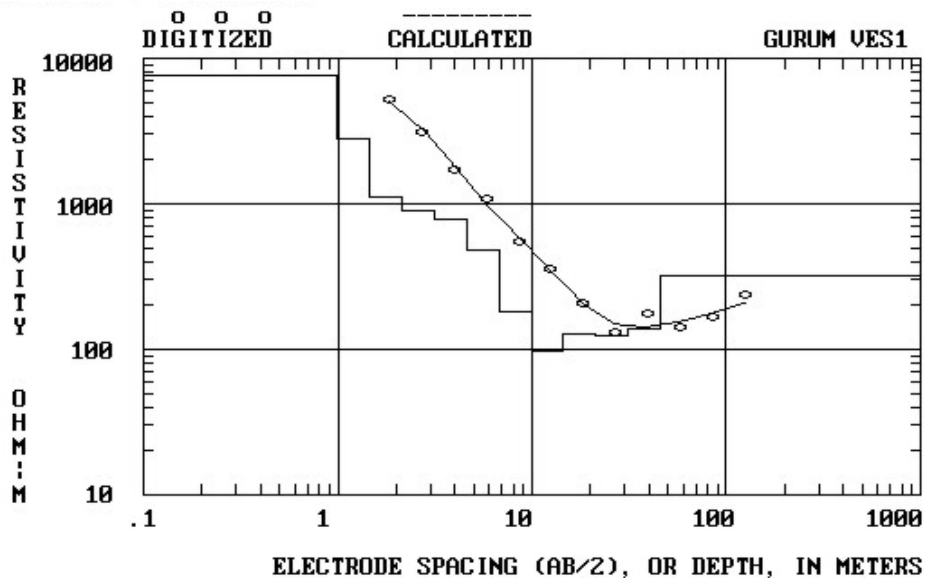


Figure 6. Geophysical Curve for VES 1

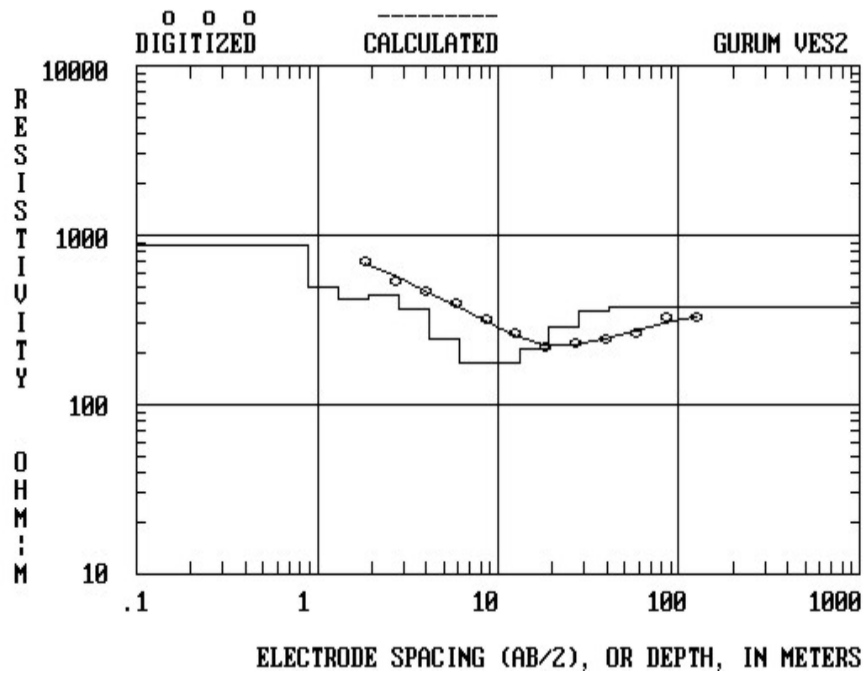


Figure 7. Geophysical Curve for VES 2

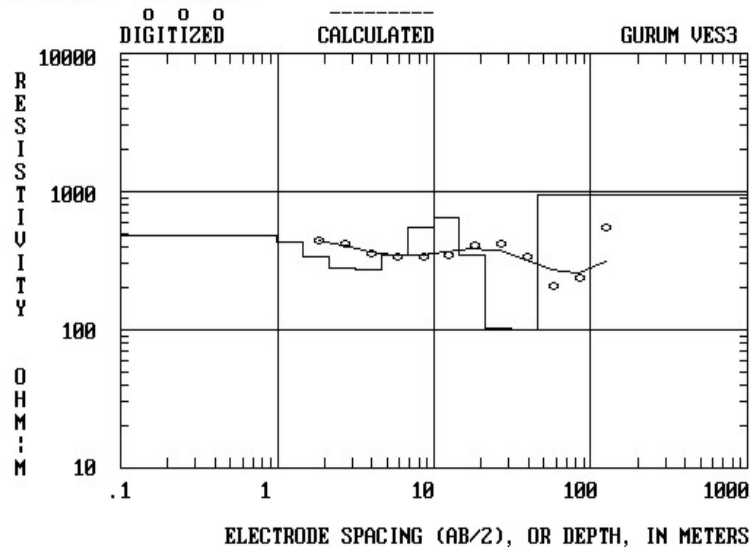


Figure 8. Geophysical Curve for VES 3

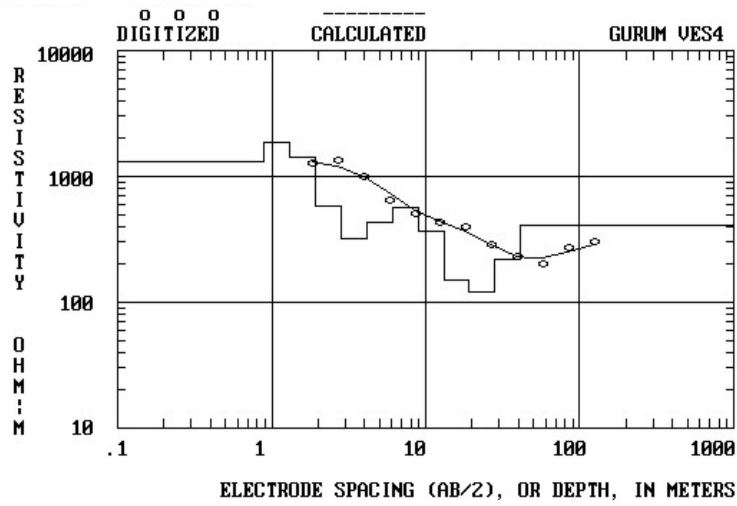


Figure 9. Geophysical Curve for VES 4

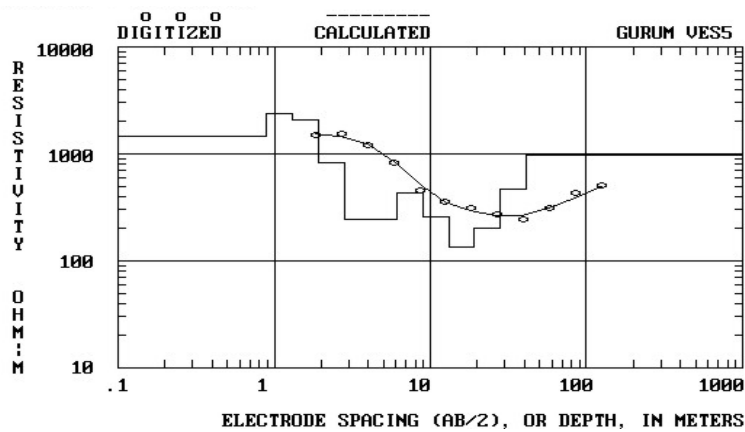


Figure 10. Geophysical Curve for VES 5

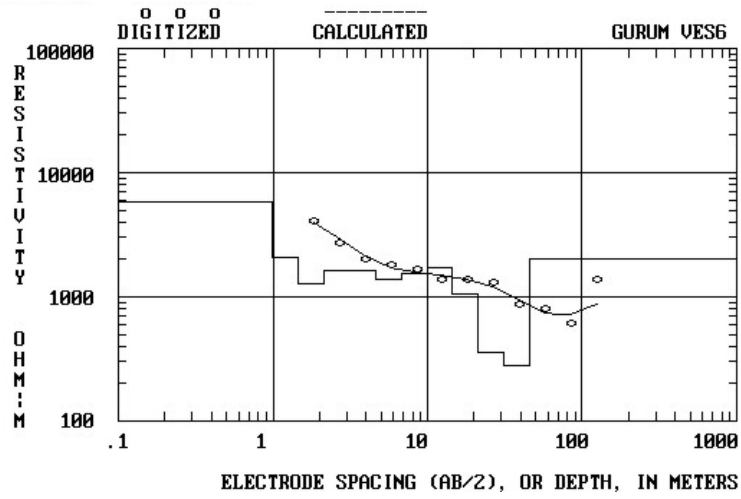


Figure 11. Geophysical Curve for VES 6

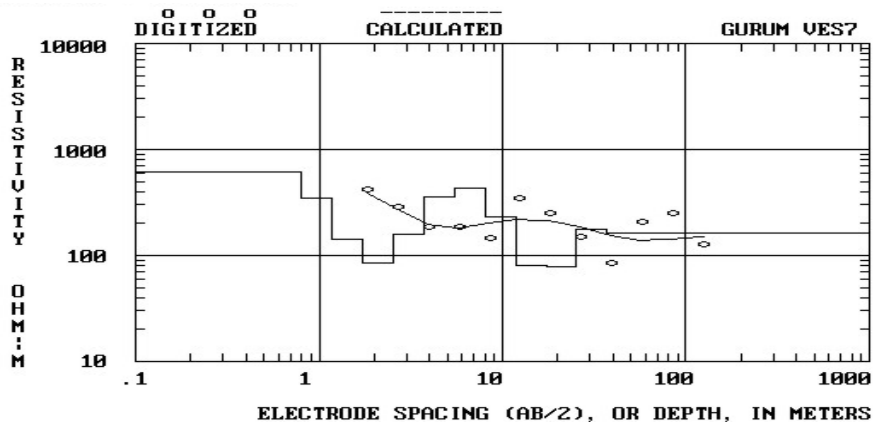


Figure 12. Geophysical Curve for VES 7

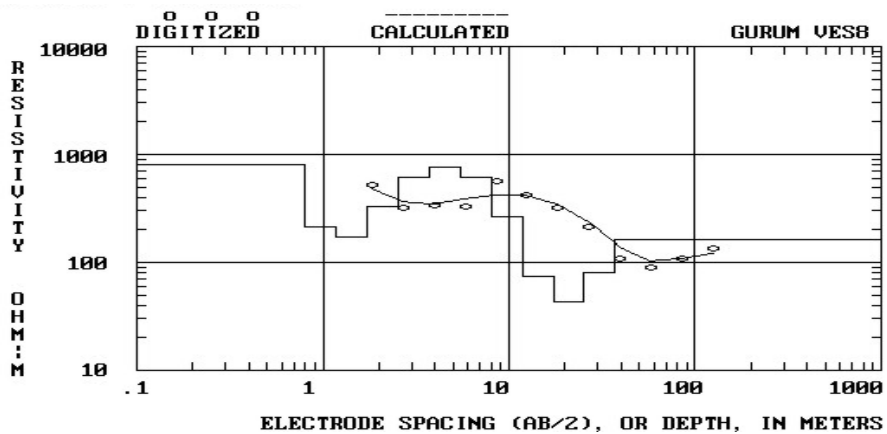


Figure 13. Geophysical Curve for VES 8

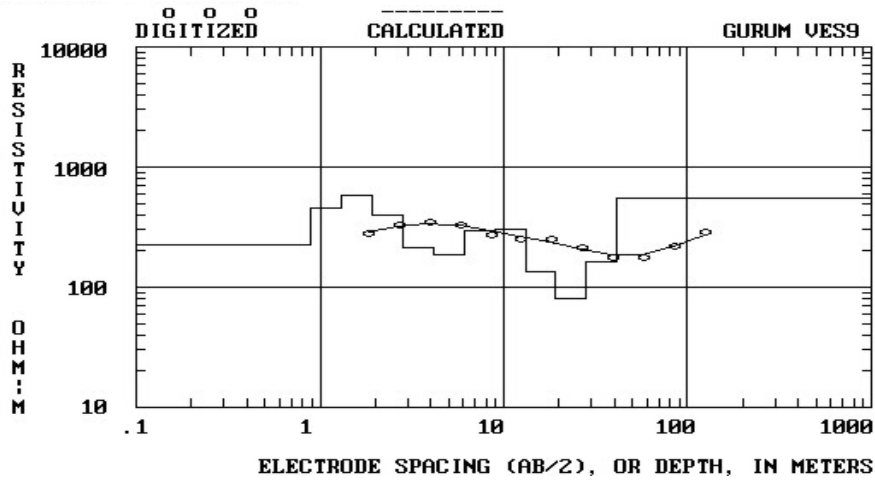


Figure 14. Geophysical Curve for VES 9

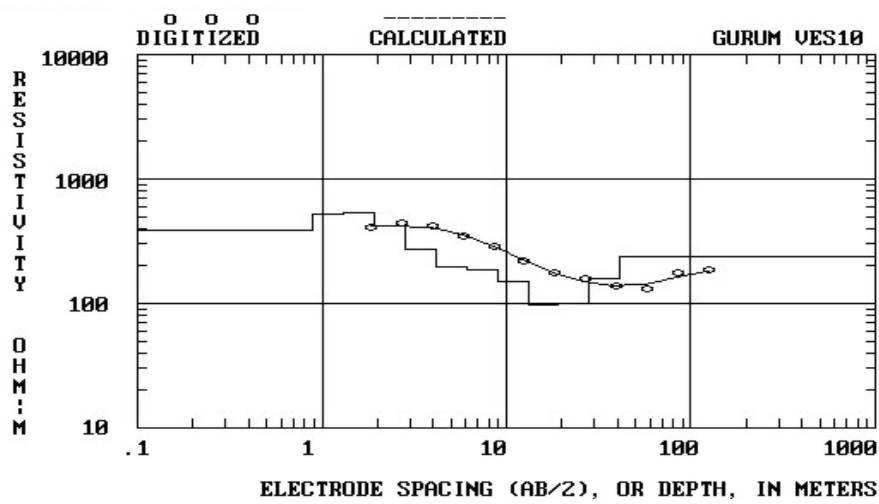


Figure 15. Geophysical Curve for VES 10

Gurum Interpreted Data

Table 13. Interpreted Geophysical Data for VES 1

Coordinates-N10° 01' 39.7"

-E008° 49' 48.1"

Elevation -1134m

Layer	Depth(m)	Resistivity(ohm/m)	Inferred litho-strata	Remarks
1	0-14.54	97.95-7712.01	Top soil	Dry
2	14.54-21.35	97.95-125.96	Laterite	Wet
3	21.35-31.38	122.58-125.95	Weathered overburden	Water bearing
4	31.38-45.99	122.58-139.61	Slightly weathered overburden	Water bearing
5	>45.99	>139.61	Slightly weathered overburden to basement	Water bearing to dry

Table 14. Interpreted Geophysical Data for VES 2

Coordinates-N10° 01' 50.5"

-E008° 49' 45.9"

Elevation -1131m

Layer	Depth(m)	Resistivity(ohm/m)	Inferred litho-strata	Remarks
1	0-1.92	422.84-879.78	Top soil	Dry
2	1.92-2.82	422.84-439.09	Laterite	Wet
3	2.82-8.92	175.76-439.09	Weathered overburden	Wet
4	8.92-41.39	175.76-359.10	Slightly weathered overburden	Water bearing
5	>41.39	>359.10	Slightly weathered overburden-fractur	Water bearing to basement

Table 15. Interpreted Geophysical Data for VES 3

Coordinates-N10° 01' 52.8"

-E008° 49' 45.5"

Elevation -1130m

Layer	Depth(m)	Resistivity(ohm/m)	Inferred litho-strata	Remarks
1	0-4.60	269.34-482.26	Top soil	Dry
2	4.60-14.54	269.34-639.97	Weathered overburden	Wet
3	14.54-45.99	99.79-639.97	Slightly weathered overburden	Water bearing
4	>45.99	>99.79	Slightly weathered overburden to basement	Water bearing

Table 16. Interpreted Geophysical Data for VES 4

Coordinates-N10° 01' 53.9"

-E008° 49' 45.2"

Elevation -1131m

Layer	Depth(m)	Resistivity(ohm/m)	Inferred litho-strata	Remarks
1	0-1.31	1320.35-1886.69	Top soil	Dry
2	1.31-4.14	320.63-1886.69	Laterite	Wet
3	4.14-8.92	320.63-570.18	Weathered overburden	Wet
4	8.92-28.20	121.44-570.18	Slightly Weathered overburden	Water bearing
5	28.20-41.39	121.44-220.36	Slightly weathered overburden	Water bearing
6	>41.39	>220.36	Slightly weathered overburden to basement	Water bearing to dry

Table 17. Interpreted Geophysical Data for VES 5

Coordinates-N10° 01' 55.5"

-E008° 49' 45.1"

Elevation -1130m

Layer	Depth(m)	Resistivity(ohm/m)	Inferred litho-strata	Remarks
1	0-1.31	1443.98-2350.63	Top soil	Dry
2	1.31-6.08	246.67-2350.63	Laterite	Moist
3	6.08-8.92	246.67-434.36	Weathered overburden	Wet

4	8.92-19.21	133.59-434.36	Slightly weathered overburden	Water bearing
5	19.21-41.39	133.59-465.87	Weathered overburden	Water bearing
6	>41.39	>465.89	Weathered to basement	Water bearing to dry

Table 18. Interpreted Geophysical Data for VES 6

Coordinates-N10° 01' 57.3"

-E008° 49' 45.3"

Elevation -1128m

Layer	Depth(m)	Resistivity(ohm/m)	Inferred litho-strata	Remarks
1	0-2.13	1279.53-5752.27	Top soil	Dry
2	2.13-4.60	1279.53-1634.31	Laterite	Moist
3	4.60-6.75	1378.26-1634.31	Weathered overburden	Wet
4	6.75-14.54	1378.26-1699.04	Slightly weathered overburden	Water bearing
5	14.54-45.99	277.69-1699.04	Fractured basement	Water bearing
6	>45.99	>277.69	Weathered to basement	W to dry

Table 19. Interpreted Geophysical Data for VES 7

Coordinates-N10° 01' 55.1"

-E008° 49' 44.1"

Elevation -1135m

Layer	Depth(m)	Resistivity(ohm/m)	Inferred litho-strata	Remarks
1	0-2.54	85.82-620.60	Top soil	Dry
2	2.54-8.03	85.82-437.65	Laterite	Wet
3	8.03-25.38	78.78-437.65	Weathered overburden	Water bearing
4	25.38-37.35	78.78-176.12	Slightly weathered overburden	Water bearing
5	>37.25	>176.12	Slightly weathered overburden to basement	Water bearing to dry

Table 20. Interpreted Geophysical Data for VES 8

Coordinates-N10° 01' 55.4"

-E008° 49' 44.1"

Elevation -1127m

Layer	Depth(m)	Resistivity(ohm/m)	Inferred litho-strata	Remarks
1	0-1.73	170.55-804.91	Top soil	Dry
2	1.73-5.47	170.55-771.55	Laterite	Dry
3	5.47-25.38	43.38-771.55	Weathered overburden	Wet
4	25.38-37.45	43.38-80.05	Slightly weathered overburden	Water bearing
5	>37.45	>80.05	Slightly weathered overburden to basement	Water bearing to dry

Table 21. Interpreted Geophysical Data for VES 9

Coordinates-N10° 01' 55.4”

-E008° 49' 47.3”

Elevation -1135m

Layer	Depth(m)	Resistivity(ohm/m)	Inferred litho-strata	Remarks
1	0-1.92	223.62-581.89	Top soil	Dry
2	1.92-6.08	186.76-581.89	Laterite	Dry
3	6.08-13.09	186.76-304.16	Weathered overburden	Wet
4	13.09-28.20	81.32-304.16	Slightly weathered overburden	Water bearing
5	28.20-41.39	81.32-160.88	Slightly weathered overburden	Water bearing
6	>41.39	>160.88	Slightly weathered overburden to basement	W to dry

Table 22. Interpreted Geophysical Data for VES 10

Coordinates-N10° 01' 55.7”

-E008° 49' 49.2”

Elevation -1135m

Layer	Depth(m)	Resistivity(ohm/m)	Inferred litho-strata	Remarks
1	0-1.92	387.76-540.19	Top soil	Dry
2	1.92-19.21	98.04-540.19	Weathered overburden	Wet
3	19.21-41.39	98.04-157.65	Slightly weathered overburden	Water bearing
4	>41.39	>157.65	Slightly weathered overburden to basement	Water bearing to dry

The interpretation of the processed data is presented in Tables 13 to 22. The tables showed depth to the various geo-electric layers and the range of apparent resistivity values for each layer. It also presents the various litho-strata or lithological units and their water yielding potentials.

From the results obtained it can be clearly stated that aquifer thickness is sufficiently thick and the resistivity values falls within the range of good water yield. It can also be said that the aquifers in the study area including both weathered overburden and fractured crystalline aquifers are capable of yielding significant amount of water to wells. Values obtained were used to plot aquifer thickness (Figure 27).

Here, the aquifer thickness appears to increase towards the north eastern part of the study area. The aquifer thickness can be said to be generally thick. The isopach map shown in Figure 27 represents the depth to basement within the study area.

To be able to see the nature of the aquifer in the area pictorially, geo-electric sections across the area have been produced. They are presented in Figures 28 to 31

Geo-electric Sections for the Study Area

Geo-electric section is a diagrammatic section of stratified layers which are deduced from electrical resistivity depth probing where layers are identified by their apparent resistivities. These sections are obtained using the interpreted results at various VES stations along the corresponding section, to obtain each section first the maximum length of each profile was taken and drawn to scale both vertical and horizontal as shown in the sections, the position of each VES point was marked out using station interval, then resistivity boundaries beneath each VES stations were located along with their thickness drawn. There are two geo-electric profiles produced for the 10 VES points. These are geo-electric section BB along VES 7 to VES

10, geo-electric section CC' along VES 1 to VES 6.

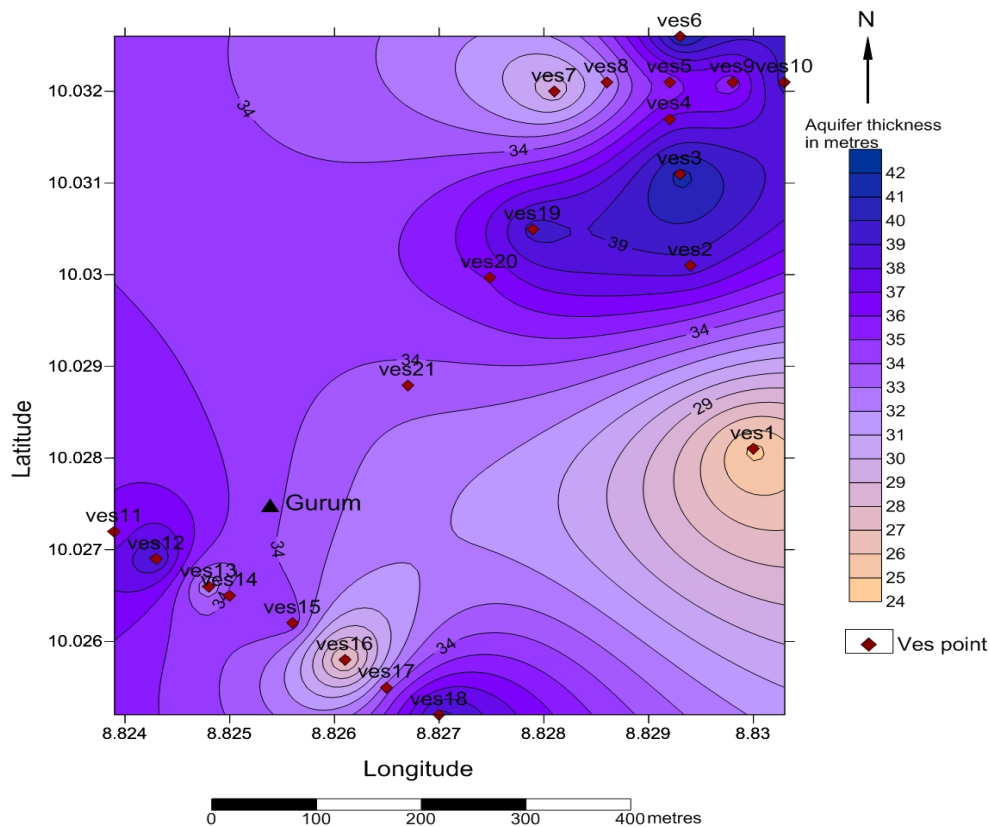


Figure 27. Aquifer thickness map of the study area

Section BB' runs across VES 5, 7, 8, 9 and 10. It covers a distance of about 270metres. The uppermost layer is the topsoil which has a high resistivity value ranging from 1443.98-170.55 ohm/metres and is composed of unconsolidated sedimentary rock unit. The second layer is composed of laterite and is present only in VES 5, 7, 8, and 9 in the geo-electric profile. It has a resistivity of about 2350.63-437.65 ohm/metres and extends to a depth of about 6.08 metres.

The third layer comprises of the weathered and the slightly weathered basement with a resistivity value ranging from 771.55-43.38 ohm/metres at VES 8. The last layer is the fresh basement with a resistivity of about 199.83-984.39.

Section CC' runs across VES 1, 2, 3, 4, 5 and 6. It extends through a distance of about 420 metres. The topsoil is composed of unconsolidated sedimentary rock with a resistivity value ranging from 1320.35-95.95 ohm/metres and extends to a depth of about 1.92 metres. Laterite underlies the topsoil with a resistivity value which ranged from 1886.69-125.93 ohm/metres and extends to a depth of 21.35 metres.

The weathered and the slightly weathered rock units are overlain by the laterite and the topsoil with resistivity of 1378.20-99.79. It extends to a depth of 45.99 metres at VES 3. The fresh basement occurs at the bottom and has a resistivity of more than 139.61ohm/meters.

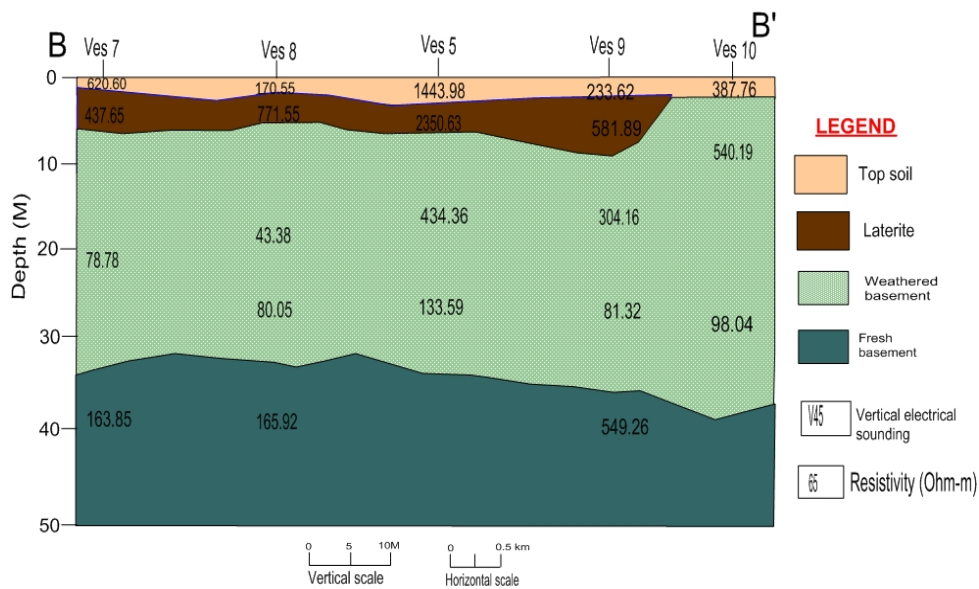


Figure 28: Geo-electric profile along section BB'

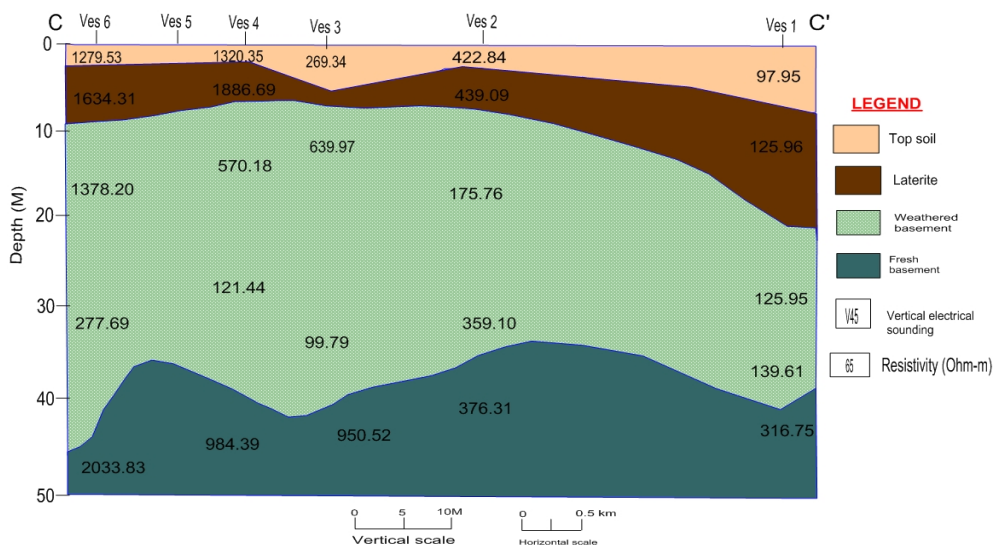


Figure 29: Geo-electric profile along section CC'

Conclusion

Geological and hydrogeophysical survey of Gurum and environs was undertaken (Lere sheet 147 SE). The area constitutes mainly of the Younger Granite and the Basement Complex rocks which were studied in details to distinguish their different lithological units in order to understand their hydrogeological potentials in the research area. The major rock units of the area are the Buji biotite granite, the applopegmatitic granite gneiss and the undifferentiated migmatites.

Multiple deformational episodes that affected the basement rock in the area gave rise to the different generation of structures observed which include foliation, joints, veins, faults and dykes.

These structures trend in the NW -SE and NE-SW directions. The structural patterns suggest that the area has been affected by widespread Pan African Orogeny. The Younger Granite rocks of the study area are closely associated with tin and columbite mineralization.

Geophysical investigation carried out here revealed that the area has good groundwater potential. The aquifers are relatively thick and the apparent resistivity values are low, meaning that conductivity is high, suggesting the possibility of good groundwater yield in most places. It can be concluded therefore that the aquifer in this area are good and can support either shallow hand pump boreholes or motorized boreholes in most places.

References

- Ajibade, A.C., Rahaman, M.A., & Ogezi A.E. (1982). The Precambrian of Nigeria. A Geochronology Summary in Precambrian geology of Nigeria. In *Geology Survey Nigerian publication* (pp. 313-323).
- Benelt, J. N. Turner, D. C, Ike, E. C. & Bowden, P. (1984). *The geology of Northern Nigeria Anorogenic Ring Complexes*. British Geology Survey overseas.
- Buchanan, M.S., Macleod, W.N & Turner, D.C. (1971). The Geology of the Jos, Plateau. *Geological survey of Nigeria Bulletin*, 32(2), 107-109. <https://doi.org/10.1038/107679a0>
- Department of Geography and Planning, University of Jos (2010- 2015). Observatory Station.
- Falconer, J. D. (1911). *The Geology and Geography of Northern Nigeria*. Macmillan London.
- Ike, E.C. (1983). The structural evolution of the Tibchi ring-complex: a case study for the Nigerian Younger Granite Province. *Journal of the Geological Society*, 140, 781 - 788. <https://doi.org/10.1144/gsjgs.140.5.0781>
- Jacobson, R. R. E., MacLeod, W. N., & Black, R. (1958). *Ring Complexes in the Younger Granite Province of Northern Nigeria*. Memoirs Geol. Soci., London.
- Koefoed, O. (1979) *Geosounding principles 1: Resistivity Measurements*. Elsevier Scientific Publication, Amsterdam, Netherlands.
- MacLeod, W. N., Turner, D. C., & Wright, E. P. (1971). The Geology of the Jos Plateau. *Bulletin of Geological Survey of Nigeria*, 3.
- Mccurry, P.M. (1971). Pan-African Orogeny in Northern Nigeria. *Geological Society of America Bulletin*, 82, 3251-3262. <https://doi.org/10.1130/0016-7606%281971%2982%5B3251%3APOINN%5D2.0.CO%3B2>
- Obaje, N G. (2009). Geology and Mineral Resources of Nigeria. Berlin, *Springer*.
- Offodile, M. E. (2002). *Groundwater Study and Development in Nigeria*. Ehindero Nig Ltd Jos.
- Offodile, M.E. (1971). *The Hydrology of the Coastal Areas of Eastern States of Nigeria*. Unpub. Geol. Survey of Nigeria, Report No. 1494.
- Olorunfemi, M.O., Ojo, J.S., & Akintunde, O. (1999). Hydro-geophysical evaluation of the groundwater potentials of the Akure metropolis, southwestern Nigeria. *Journal of Mining and Geology*, 35, 207-228.
- Turner, D.C. (1976). Structure and Petrology of the Younger Granite Ring Complexes in *Geology of Nigeria*, edited by C.A. Kogbe, Rockview (Nigeria) Ltd.
- Wright, E. P., 1971. The Basement Complex. *Bulletin Geological Survey of Nigeria*, 32, 12-47. http://dx.doi.org/10.1007/978-3-540-92685-6_2
- Zohdy, A.A.R, Eaton, G.P., & Mabey, D.R. (1974). *Application of surface geophysics to groundwater investigations*. Collection of Environmental data published by the Department of the Interior Geological Survey.